Computers, Environment and Urban Systems 62 (2017) 99–112

Contents lists available at ScienceDirect

Computers, Environment and Urban Systems

journal homepage: www.elsevier.com/locate/ceus

Putting people in the picture: Combining big location-based social media data and remote sensing imagery for enhanced contextual urban information in Shanghai

Michael Jendryke [a], Timo Balz [a,b,*], Stephen C McClure [a], Mingsheng Liao [a,b]

[a] State Key Laboratory of Information Engineering in Surveying, Mapping and Remote Sensing, Wuhan University, 129 Luoyu Road, Wuhan 430079, China
[b] Collaborative Innovation Center for Geospatial Technology, 129 Luoyu Road, Wuhan 430079, China

ARTICLE INFO

Article history:
Received 29 March 2016
Received in revised form 8 October 2016
Accepted 8 October 2016
Available online xxxx

Keywords:
Geography
Remote sensing
Sina Weibo
Social media
Urbanization

ABSTRACT

Urbanization is a set of interrelated processes; the most visible among them are changes in the built-up environment. We relate those changes to human activity as expressed by online social media messages. This approach might shed light on urban dynamics currently intractable through existing datasets and methodologies. Microwave remote sensing images are used to identify urban built-up areas and changes within those areas in an objective way, while geocoded mobile social media messages deliver valuable information about human activity and the vitality found in those areas. A time-series stack of 36 TerraSAR-X Stripmap images and roughly six million social media messages were processed, classified, and visually and quantitatively analyzed for an experiment in Shanghai. We derived four possible cases of land classification by combining the results of both sources to a single raster layer at a 400 m cell size. Quantifying these cases in a 2-by-2 confusion matrix shows positive and negative matches between built-up areas and social media messages. We see that correlation of positive matches is 72%. A combination of remotely sensed and social media data is a step towards a more granular analysis of urbanization processes than is possible from either data source alone. We put people in the picture of traditional remote sensing analysis.

1. Introduction

Urbanization is observable in developing and developed countries. In today's world, more than half of the Earth's population lives in cities, The United Nations Organization World Population Report shows that >50% of the global population lives in urban areas already (United Nations Population Division, 2011). In China by 2030, one billion people are expected to be living in cities; this is far >50%. In this paper, we will focus on the urbanization process in China; in particular, on the detection of built-up areas and human activity in Shanghai (SH) using Synthetic Aperture Radar (SAR) data and location-based Social Media Messages (SMM), bypassing official data sources entirely, for a more objective understanding of these urbanization processes.

We argue that the combination of SAR remote sensing and location-based social media messages can enhance land classification and interpretation of urban development and human activity patterns. Remote sensing identifies urban built-up areas; social media messages are an indicator of human activity in a given area. We show that it is possible to identify 'high' and 'low' built-up areas as well as human activity patterns from each data set. Overlaying and classifying SAR and SMM results generated four possible classes/cases of land-cover.

We used a stack of TerraSAR-X images collected over Shanghai for our experiment. Microwave remote sensing is an objective (Lillesand, Kiefer, & Chipman, 2015) and deterministic (Woodhouse, 2006) imaging system; recording two images under exactly the same conditions will produce identical images, but variations occur due to system noise. Moreover, sensor selection and parameter settings for an image acquisition, such as spatial resolution or time of recording and interpretation of results are subject to human bias. One image represents a single snapshot of the current situation on the ground. A stack of images over the same area delivers a time series. Each time the satellite passes over an area of interest (AOI), it can be observed from almost the same position, creating a time series of image observations; for TerraSAR-X the repeat cycle is 11 days. Every image, therefore, has almost identical properties and thus is suitable for performing Coherence Change Detection (CCD) to monitor changes on the ground.

Microwave remote sensing is useful for identifying urban built-up areas and changes within these areas. Urban areas have buildings, roads, construction, general infrastructure, and paved ground with steel, glass concrete and stone objects. From a technical perspective, these *high coherence* objects appear to be phase coherent in a SAR

* Corresponding author at: State Key Laboratory of Information Engineering in Surveying, Mapping and Remote Sensing, Wuhan University, Wuhan 430079, China.
E-mail addresses: michael.jendryke@rub.de (M. Jendryke), balz@whu.edu.cn (T. Balz).

http://dx.doi.org/10.1016/j.compenvurbsys.2016.10.004

image pair. Because they usually do not move, these objects are considered stable. We define these as built-up areas.

Human activity, in this study, is represented by SMM with geographical coordinates and timestamps. We define human activity as the existence of social media messages (points) within a given area – a grid cell (raster). To post a message, users must interact with a mobile device that signals its current GPS location back to the social media network. This is, in essence, an indication of human activity from one individual at a geo-location. Collecting millions of messages in a municipal area gives us a more general picture of the human activity patterns across the entire city and variations within; from the center, down to small towns (zhen - 镇) and even smaller units, like the Oriental Sports Center or the Pudong International Airport in Shanghai.

Section 1 starts with a discussion of our motivation and continues with a review of the published research relevant to our study. Section 2 describes the big data sets from remote sensing and social media as well as their retrieval. The methodologies to derive and quantify the built-up area from SAR and the inference of human activity from social media messages are detailed in Section 3. Change detection within urban areas and the patterns of human activity are discussed in Section 4. This section also includes an analysis of the combined classifications of both data sets. In Section 5, we draw conclusions, address the limitations of this research, and outline our future research directions.

1.1. Motivation

The contentious socio-political context must be considered when investigating land use patterns and human activity, especially in China. Given their controversial political or commercial nature, the data documenting urbanization are often not trustworthy, reliable, inaccessible, or in many instances, they are outdated. For example, census data is not available for neighborhoods and the data that is accessible, is irrelevant to an understanding of rapidly changing urban dynamics (Taylor, 2001). The census data for the townships in the Shanghai metropolitan area consists of only 235 points (China Data Center, 2013), which is a rather coarse positional accuracy.

The motivation for this study was a need for an enhanced and timely analysis of urban processes in Chinese cities. Structural change and population dynamics as measured by two seemingly unrelated big data sources can be integrated using visual overlaying techniques and quantified through classification. A geographical analysis is possible since both data sets have the same reference system. These data can augment, or bypass traditional data sources for a reliable and less contentious source of data about Chinese cities and complex urban processes.

Microwave remote sensing is a weather and daylight independent image acquisition system. It can provide time-series image stacks that are particularly suitable for detecting and identifying small and large-scale changes in the built environment. Due to its relative independence from atmospheric distortions, SAR delivers more stable time-series imagery than optical imagery. This capacity to create consistent time-series images irrespective of cloud coverage is a major advantage of SAR imagery when the goal is to detect urban change happening over short time intervals (weeks). SAR is an objective and independent system. Thus, determining a built-up urban footprint or the building density become purely technical questions rather than issues influenced by political or commercial interests. SAR or any other space-borne remote sensing imagery, however, does not provide information about direct human activity. People are not visible or classifiable in an image unless the resolution is very high or taken from an air-borne sensor.

Social media messages are a readily available and timely means to quantify and measure human activity particularly A point cloud, gathered from a location-based social media network is one possible data source useful for discerning human activity in a small area. This social media activity might or might not be directly linked to changes in the built-up environment.

The development of built-up spaces and human activity are not always congruent and simultaneous. This leaves uncertainties when only looking at remote sensing data that can be used to classify an area as urban by just looking at built-up structures ignoring the fact that something becomes urban with the presence of people. Patterns arise that are concurrent, shifted in time or never overlapping as shown in Table 1. Example: An area can have a high degree of urbanization on the structural level, but people are not living there leaving the environment in a state similar to a 'ghost town'.

Social media messages give us a representation or albeit a limited, picture of human activity occurring on the ground and can augment the view from satellite cameras or remote sensing devices. Social media is partial and limited, leaving large areas of uncertainty. We are restricted to people from a society with a strong technological orientation who also use Sina Weibo on a mobile device with the reception of location information. This allows us to capture human activity at any time of the day for a single individual. We are focused on human activities as measured by messages on social media per area unit, not in the exact number of people per area unit. The issue we address are urban processes occurring at two scales, change occurring in the larger built environment and the activity patterns represented by aggregated SMM from individuals.

1.2. Literature review

This study is a contribution and a tool for urban planners and designers as well as scientists dealing with spatial information from various sources to observe urban processes. The literature that has been reviewed comes from two major fields of research: a) urbanization as seen from space (remote sensing) and b) urban processes such as human activity (inferred from social media). An approach that fuses both research fields directly was published in Liu et al. (2015). The author describes the similarities of representation and analysis of remote sensing imagery and data gathered from human activity (taxi trajectories and check-in data from social media) and calls this type of research social sensing.

1.2.1. Remote sensing

Remote sensing plays an important role in China's urban planning process (Esch, Taubenbock, Felbier, Heldens, Wiesner & Dech, 2012; Xiao & Zhan, 2009). There have been studies on the subject of urban change using satellite data from microwave sensors (Liu & Yamazaki, 2011) to detect urban changes using amplitude (Boldt & Schulz, 2012)

Table 1
Basic schema for visual classification: Density of built-up and density of social media messages lead to four possible cases.

Social Media Messages \ Built-up area	high	low
high	Case 1: e.g. CBD	Case 2: e.g. a park
low	Case 3: e.g. industrial area	Case 4: e.g. agricultural land

and phase (Chi, Sun, & Ling, 2009; He & He, 2009) information assisted by optical data. Detecting changes in land subsidence and building height at the millimeter and meter levels are discussed in Brunner, Lemoine, Bruzzone, and Greidanus (2010), Perissin and Wang (2011). They describe specific applications for urban areas whereas others are basically interested in the two-dimensional extent of an urbanized area for further applications (Jin, Kessomkiat, & Pereira, 2011). Research to identify urban areas with InSAR, not only in 2D but also in height (buildings) was demonstrated in Brunner et al., (2010) and might be of value in our approach.

In a broader global context of urbanization and population estimation studies, SAR systems are frequently used to identify human settlements, as in Esch et al. (2013), Esch, Taubenböck, Roth, Heldens, Felbier, Thiel, et al. (2012) and Yifang, Alexander, and Gamba (2013). Satellite data capturing night-time lights is used for population estimation, this approach with DMSP OLS is described in Sutton, Roberts, Elvidge, and Baugh (2010), Li and Li (2014) and Huang, Yang, Gao, Yang, and Zhao (2014). Nighttime lights are an indirect measurement as they cannot be linked to individual behaviors. However, in our study, we are not estimating population with social media. Instead, we use social media data to infer human activity thus adding richness to remotely sensed imagery.

1.2.2. Social sensors

Social sensor datasets include taxi trajectories within urban areas (Ding, Fan, & Meng, 2015; Liu, Wang, Xiao, & Gao, 2012), and social media check-in data (Liu, Sui, Kang, & Gao, 2014) between cities. The most popular dataset, however, seems to be mobile phone/cellular phone call data as shown in Calabrese, Colonna, Lovisolo, Parata, and Ratti (2010), Calabrese, Diao, Di Lorenzo, Ferreira, and Ratti (2013), Candia et al. (2008), Gao (2015), Kang, Sobolevsky, Liu, and Ratti (2013), Liu et al. (2012), Louail et al. (2014), Reades, Calabrese, Sevtsuk, and Ratti (2007), and Reades, Calabrese, and Ratti (2009). Individuals often do not voluntarily share mobile phone data, and it is difficult to obtain this kind of data from network providers. Social media data is a form of Volunteered Geographic Information (VGI), where citizens act as sensors (Goodchild, 2007). We believe that this data – voluntarily shared by a subset of the population – can indicate human activity patterns in a way similar to cell phone usage, see Calabrese et al. (2010) and references above.

Exploration of the semantic content in social media is an active area of research, to identify places, narratives, and functions of an urban area as presented in Crooks et al. (2015), Jenkins, Croitoru, Crooks, and Stefanidis (2016), and Lansley and Longley (2016). Social network data can deliver information on many different topics e.g. bullying (Carter, 2013), health related issues (Guo & Goh, 2014; Widener & Li, 2014), word of mouth studies (Rui, Liu, & Whinston, 2013), emergency locations (Ao, Zhang, & Cao, 2014), military operations (Kase, Bowman, Al Amin, & Abdelzaher, 2014), and social activity hotspots (Stefanidis, Crooks, & Radzikowski, 2013). This research is only of marginal relevance to our work but illustrates the broadness and depth of information that can be extracted from social media. We, however, are not analyzing the content or the semantic meaning of a message text, but rather consider only the geo-location of a message to enhance and augment traditional remote sensing for urban change monitoring.

1.2.3. Limitations and possibilities of social sensing

Ruths and Pfeffer (2014) show issues that have to be addressed by researchers when dealing with big social media data sets. In 2009, Google started the Google Flu Trends (GFT) project utilizing a prediction algorithm and big social media data; a black box for social media data yielding inaccurate predictive results not subject to scrutiny or replication (Lazer, Kennedy, King, & Vespignani, 2014). Other papers highlight the pitfalls and difficulties of social media big data (Cohen & Ruths, 2013; Tufekci, 2014): Dominance of one network alone instead of comparing with other networks (Chen et al., 2011), not considering the user sampling bias or not surveying the network (Fu & Chau, 2013) or semantic searches by e.g. 'hashtags'. Neglecting these could lead to false interpretations.

According to Broniatowski, Paul, and Dredze (2014) however, big data from social media (e.g. Twitter) can be used for analysis because replication, filtering, and inherent system biases can be overcome when these data sets are openly accessible (e.g. API) and researchers are clear about the limitations (Ruths & Pfeffer, 2014) of these data. These limitations lie within the flawed nature of social media data; therefore, it is necessary to reduce biases during the collection and methodological handling. Quantifying population biases, comparing between two networks or the same network at different times might mitigate these flaws according to a list in Ruths and Pfeffer (2014).

A user has to employ a GPS enabled device and use the Sina Weibo application for Android or iOS to embed location information as GPS coordinates in the metadata of the message. The web interface does not have the option to attach GPS coordinates; a user must spell out the name of the place in the message text e.g. 'Shanghai', 'the Bund' to represent their location. This kind of location information could only be harvested through a semantic search as suggested in Burton, Tanner, Giraud-Carrier, West, and Barnes (2012). The API request *nearby_timeline( )*, that we used only returns messages with a GPS coordinate pair in decimal degrees (with five decimal places).

2. Experimental data sets for the Shanghai study area

The initial data set in our study was a stack of 36 single look complex (SLC) TerraSAR-X Stripmap images with a wavelength of 3.1 cm in VV polarization covering the center and surrounding areas of Shanghai. The image stack was collected from 2008 to October 2012.

The social media network data was harvested from Sina Weibo, similar to Twitter (Chen et al., 2011). This web-based network has an asymmetric user structure (i.e. every user can follow anyone else without establishing a mutual friendship connection) and includes location information. Sina Weibo is used on both stationary and mobile devices with GPS. A user can activate a feature to attach geographical coordinates to messages. This is an opt-in option. For our experiments, only messages with geographical coordinates attached were used. Similar to Twitter, Flickr, and Instagram, Sina Weibo users can follow each other to share public and private content such as text and pictures. All messages were downloaded free of charge through an open API (Application Programming Interface) that can be accessed after creating a profile on Sina Weibo.

A study by Fu and Chau (2013) discusses Sina Weibo network usage statistics; in an analysis of a random sample of ~30,000 users, they found that most profiles are actually empty and without message content. Sina Weibo users are concentrated in areas along the southeast coast, Beijing and Tibet, as shown in Fu and Chau (2013). About 13% of the users in this sample produced one message per week, while 4.8% of all users produced 80% of the content. Thus, the more followers someone has the more likely they produce original content.

The limitations raised by Ruths and Pfeffer (2014) also apply to our data set. A) Biases are introduced by the Sina Weibo platform itself. These include the filtering of 'old' messages and the preference of messages from so-called VIP-users. We have no information how these algorithms work. B) At this point we also have no knowledge about who is using the network (e.g. gender ratio and age), and if/how their behavior in the 'online world' differs from the 'offline world' (Zook & Poorthuis, 2014). The collected message points are not a representation of the network or the population; inferring the true population information for an area is intractable at this point. C) Repeatability: Due to the limitations mentioned in a) an identical data set could most likely not be reproduced, but a similar data set could be generated using the method described in this paper.

A drawback of the presented approach is due to the non-concurrence of the remote sensing imagery and the social media messages.

The time gap between both datasets is two years, which leads to two possible scenarios: a) An area that is identified as built-up may be undergoing development (less stable coherence signature, see Chapter 3.1) by the time of message collection or b) a construction (again less stable coherence signature) was detected at the time of image acquisition, but was actually finalized by the time of SMM collection.

The errors that arise from the non-concurrence are unfortunately not avoidable with the current data. While it would be preferable to have data that covers the same period, the introduced uncertainties in the combined and aggregated dataset have to be mentioned and accepted. Changes in the built-up environment have certainly occurred, but are not detected due to the lack of data. The population grew from 23,804,300 (14,269,300 SH residents) in 2012 to 24,256,800 (14,386,900 SH residents) in 2014; a 1.9% (0.8% SH residents) increase (Shanghai Bureau of Statistics, 2015, chap. 2.1). This may result in different population patterns that do not fit the built-up information of 2012 detected by SAR imagery. The error that is present in the final result is due to built-up information from 2012 and human activity information from 2014.

3. Methodology

The methodology is split up in two (independent) processes, the generation of coherence images to identify built-up, and the gridding of Social Media Message (SMM) points into a raster that shows areas of human activity. The results are combined into a single layer. The process flow is outlined in Fig. 1 and explained in the following sections. The time series stack of SAR images is processed using a Small BAseline Subset (SBAS) approach, not Single Master (SM), see Section 3.1 below. From these images, a selection is averaged over time and space. The result can be a single image or a time series of multiple images, which are then classified by applying a threshold of coherence >0.5. Social media messages processing is done separately. It starts with the collection of the messages, which is a process in itself. Each message resembles a point, which has a number of attributes. For each squared grid cell, the count of messages within this area is stored (gridding). As described in Section 3.2 this human activity layer is then classified before it is combined with the results from the built-up area classification (see Section 3.3).

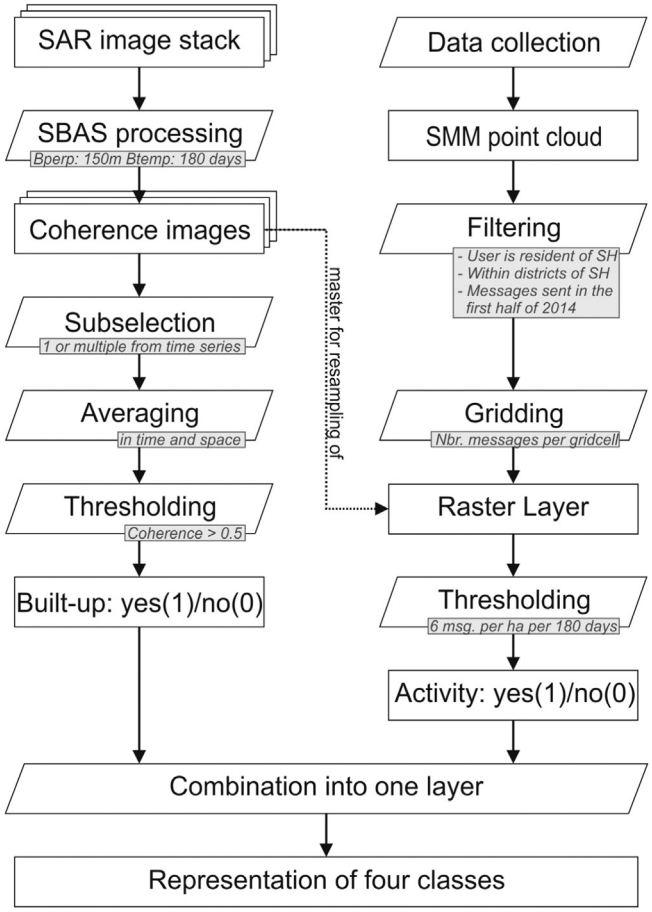

Fig. 1. Flow chart of the methodology.

3.1. Deriving built-up areas from SAR coherence

Urban areas are often characterized by concrete structures and buildings with less water and vegetation. High buildings cause layover and shadow effects, especially in dense urban areas that make the separation of objects difficult or impossible. Built-up areas appear with higher intensity backscatter and a stable phase attitude. The condition for a stable phase attitude is that the entire built-up object is not moving in any direction. Phase stability is also termed phase coherence. Phase stability measurement can provide an indication whether the land is covered with buildings and man-made structures or not.

The words coherence and correlation are used interchangeably in the context of this paper. Decorrelation is caused by the relative phase difference in the distance between two observations – different phase angles. The following is a list of possible reasons for phase decorrelation.

- Phase decorrelation due to atmospheric effects. The atmosphere and especially the water vapor in the lower atmosphere can cause a phase delay (Wadge, 2002).
- Phase delay due to ionospheric effects (Xu, Wu, & Wu, 2004).
- If the ground is subsiding/raising or moving in any way in relation to the line of sight to the satellite, then the distance changes and the phase becomes incoherent:
  - o Long term (years) changes like ground subsidence caused by e.g. extraction of groundwater, petrol or slow-moving landslides.
  - o Short term (seconds/min) changes such ruptures occurring as a result of e.g. earthquakes.
- Variations in the water content/humidity of soil/earth
- Vegetation and water are incoherent due to constant influence by wind
- The observed phase is also influenced by the satellite system itself, more precisely the temporal (B_{temp}) and perpendicular (B_{perp}) baselines between two observations. If one or both baselines are too large than the phase decorrelates.

Construction sides appear incoherent. This is a very important attribute when it comes to change detection within urban areas. Three possible scenarios can easily be identified in SAR coherence change detection:

a) The land is covered with vegetation such as agriculture and is converted to a built-up environment. Here we see a change from incoherence towards high coherence.
b) The land is covered with buildings that are destroyed to make space for new constructions. This appears coherent in the image with a time period of incoherence in between.
c) From buildings to vegetation: This process is also observable when urban land is transformed to forest.

These cases are a strong generalization and ignore the situation when naturally stable land (such as rocks) is changed to built-up area.

From all available input images, we combined those with a temporal baseline (B_{temp}) of <180 days and a perpendicular baseline (B_{perp}) of <150 m – similar to an SBAS approach. With these settings, we created

109 coherence images out of 36 SLC images. A longer time separation would lead to too much temporal decorrelation. The phase coherence is also affected by the orbit separation; therefore, we exclude pairs with perpendicular baselines of >150 m.

All combinations are processed to ten mean coherence images (adding 10 to 14 subsequent images together). This gives a stack with ten bands where each band resembles a certain timeframe. Three bands of this stack are visualized in an RGB composite. Color coding coherence measurements at different times in a single RGB composite makes it easier to detected and understand changes (see Chapter 4.1 Fig. 3).

3.2. Human activity inferred from social media messages

In this study, we demonstrate a method to derive and quantify human activity in urban areas. There are many ways to count the population within a city district, such as census information but this information is collected for a different purpose and not available to us and only represents a snapshot in time. Social media messages, however, when sent from mobile devices with geographical coordinates added, delivers accurate time and location information.

We define human activity as a message that is sent through the Sina Weibo application with Meta information about time and location attached (the timestamp is precise to milliseconds, set by the Sina Weibo system, and cannot be altered). Due to the nature of the exploited API request, it is highly likely that the message has been generated using a mobile device. There is no option to infer the current activity without a semantic analysis of the message content, human activity is a geographic point sent by a user identification number with a timestamp.

All received messages are pre-filtered to avoid suspicious user accounts with: a) users with an average of 20 messages per day, b) users that have 26 weeks (half year) with >60 messages, and c) only one message in the profile at all (those accounts are probably only created to sell followers). These restrictions are set based on the distribution of messages per account – a sharp decline of the number of messages is noticeable. An additional filter only selects messages from users that entered in their profile information, that they reside in Shanghai, and sent messages between January and June 2014. Only Monthly Active Users (MAU) were included; users with at least one message per month. This left a total set of 3,629,865 message points for the Shanghai municipal area.

We used the query *nearby timeline()* (Sina Weibo, 2014), a spatial query, with a center coordinate and a search radius of up to 11,132 m. This query only returns messages with GPS coordinates in decimal degrees. Further possible query options include the definition of a

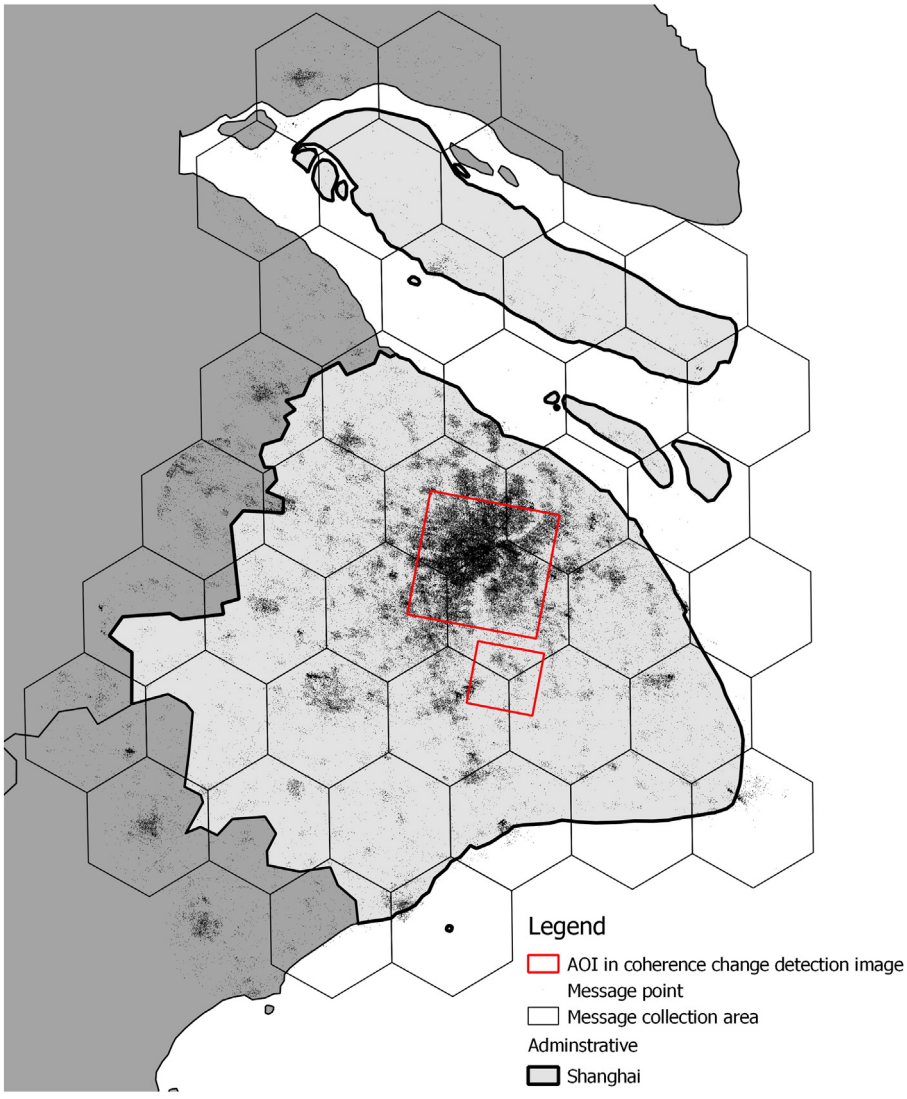

Fig. 2. Each query uses a center coordinate and a search radius to collect the message; in this schematic map a center and its area are shown as hexagons. The hexagons are used for internal statistics during the message collection process.

timeframe; the system will only return messages sent in that period. We harvested messages that cover the area of Shanghai from January to June 2014 using 38 center coordinates. The 5.8 million geocoded messages collected include 36 attributes and are stored in a MySQL database. Fig. 2 shows the center coordinates and their area (visualized as hexagons) for the queries. The hexagons cover the entire area of Shanghai; the red squares represent the processed SAR coherence image stacks.

An excerpt of the C# code to call this API request is shown below. The returned result is a JavaScript Object Notation (JSON) string. This string has to be parsed and parameterized before it is sent to the database. The parameters are the geographical latitude and longitude coordinates and time stamps in UNIX time.

```
1:  NTL = Sina.GetCommand("https://api.weibo.com/2/place/nearby_timeline.json",
2:        new WeiboParameters("lat", '31.150938'),          // Latitude
3:        new WeiboParameter("long", '121.752096'),         // Longitude
4:        new WeiboParameter("range", '11000'),             // maximum radius
                                                            is 11132m
5:        new WeiboParameter("starttime", '1388534400'),    // Starttime (UNIX)
6:        new WeiboParameter("endtime", '1404172800'),      // Endtime (UNIX)
7:        new WeiboParameter("sort", false),                // sort
8:        new WeiboParameter("count", '50'),                // max. number of
                                                            records returned
9:        new WeiboParameter("page", '1'),                  // pages
10:       new WeiboParameter("base_app", false),            // API variable
11:       new WeiboParameter("offset", false));             // API variable
```

3.3. Establishing common ground

Both data sets are independent and independently processed, but they do have a common spatial reference system. This common spatial reference allows us to superimpose the data sets. These layers are represented as rasters with the same coverage when the message points are aggregated to a grid. An overlay reveals urban dynamics such as long-term changes in the built-up development as well as human activity within or outside these areas.

We regard urban dynamics as the combination of processes of structural change and human activity. This is illustrated in Table 1: If an area is dominated by built-up structures and we detect a large volume of SMM, then this intensely used built up area will be classified/categorized as case one, and could potentially be a central business district or a shopping area with malls or other attractions. An area with less built-up density, few to no buildings and a large volume of SMM, classified/categorized as case 2, might indicate a park like area. However, if only the number of recorded SMM drops and not the built-up density, we may have identified an industrial area, case 3. The absence of infrastructure and a low volume of SMM, case 4, might indicate agricultural or forested land. Here we are not attempting to classify land use patterns, the examples stated above and in Table 1 are suggested possibilities and are not to be determined with this method.

To quantify and extend a visual interpretation of this data, we resampled and classified both rasters. Both data sets have a common spatial reference, representing a 2-dimensional area. We established unity by aggregating both data sets to square cells with an edge length of 400 m. A

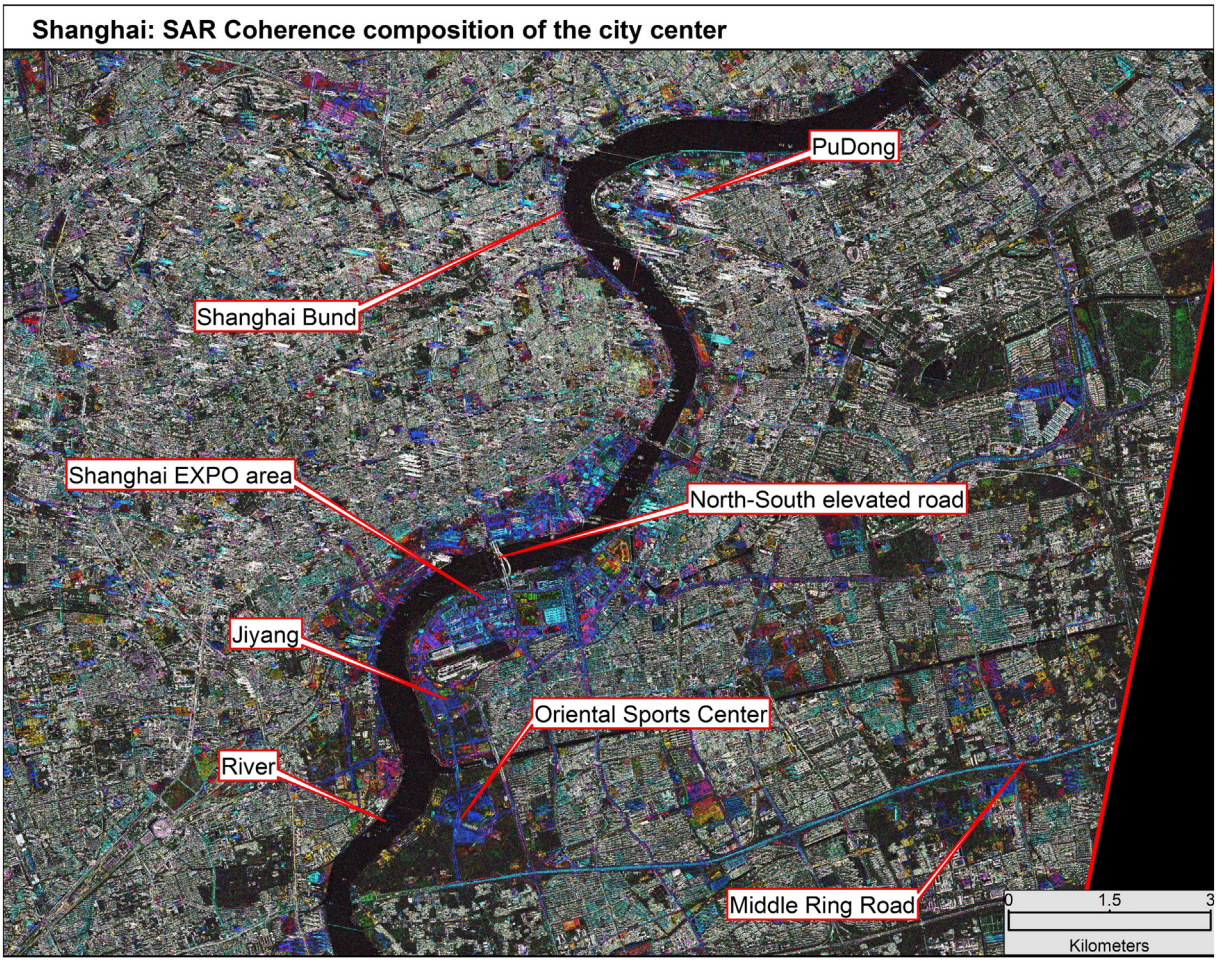

Fig. 3. RGB Color composition of coherence change detection in Shanghai. Band 1 is red and resembles the period in spring 2009, Band 2 is green and constitutes the time of end 2009 to end 2011 and Band 3 is blue for 2012. (For interpretation of the references to color in this figure legend, the reader is referred to the web version of this article.)

threshold of 0.5 was applied to the coherence layer to derive two classes of built-up or non-built-up areas (0/1). The volume of social media messages per cell was used to classify them as either human activity or not active areas (0/1), by applying a threshold of six messages per 180 days per hectare. This threshold is established as a correspondence to 'monthly active users' Four possible classes are derived as shown in Table 1. With this basic binary classification, we can identify areas that are

- built-up with human activity (1, 1),
- not built-up and have no human activity (0, 0),
- built-up without human activity (1, 0), and
- not built-up with human activity (0, 1).

To identify if there is scale dependence we iterate different coherence thresholds [0.40, 0.425, 0.45, 0.475, 0.5, 0.525, 0.55, 0.575 and 0.6] against different message counts (1 to 40 messages per hectare per 180 days) for various grid cell sizes of [100, 200, 250, 400, 500, 800, 1000, 1600, 2000] meters. The 400 m cell size has been selected because it delivers the highest matching for a coherence threshold of 0.5 (best classification of built-up) and a reference number of 6 message per hectare per 180 days (similarly to monthly active users).

Built-up areas represented as a raster layer and social media messages represented as a point cloud cannot be directly compared. When both data sets are represented as raster grids at the same resolution, they can be evaluated for patterns of correlation and spatial autocorrelation between built-up and human activity areas.

4. Results and discussion

4.1. Urban infrastructure change detection

The principle result of the analysis of 36 SLC images is urban land cover change detection for two areas in Shanghai. Fig. 3 shows the first area in the center of Shanghai, generated by combining three mean coherence images to an RGB composite. Color-coding makes the changes over time apparent. Dark areas in an image indicate incoherence. The HuangPu river that runs through the scene, for example, is dark because it is in motion and unstable in comparison to the wavelength of the sensor. Also in Fig. 3, we can see bright patches and strips in the Shanghai Pudong area. Those are high-rise buildings, built before 2009. They show up as white because no change happened to these structures. No change means that no changes on the facade occurred and the building itself did not move. However, there are also blue color pixels visible within this area that indicates change over time.

The blue color code was assigned to band 3, which represents the year 2012. High coherence in this year is depicted in blue for the whole image. The interpretation is that this building was constructed right before, or the scaffolding was removed, in 2012. This is also true for the large blue area in the center of the scene. This is the old world exhibition area of 2010. The construction of the pavilions ended in early 2010. Today this area is unused. Changes like this can also be seen along the middle ring road, in Jiyang and the Oriental Sports Center which was constructed between late 2008 and late 2010 (Fédération internationale de natation, 2010).

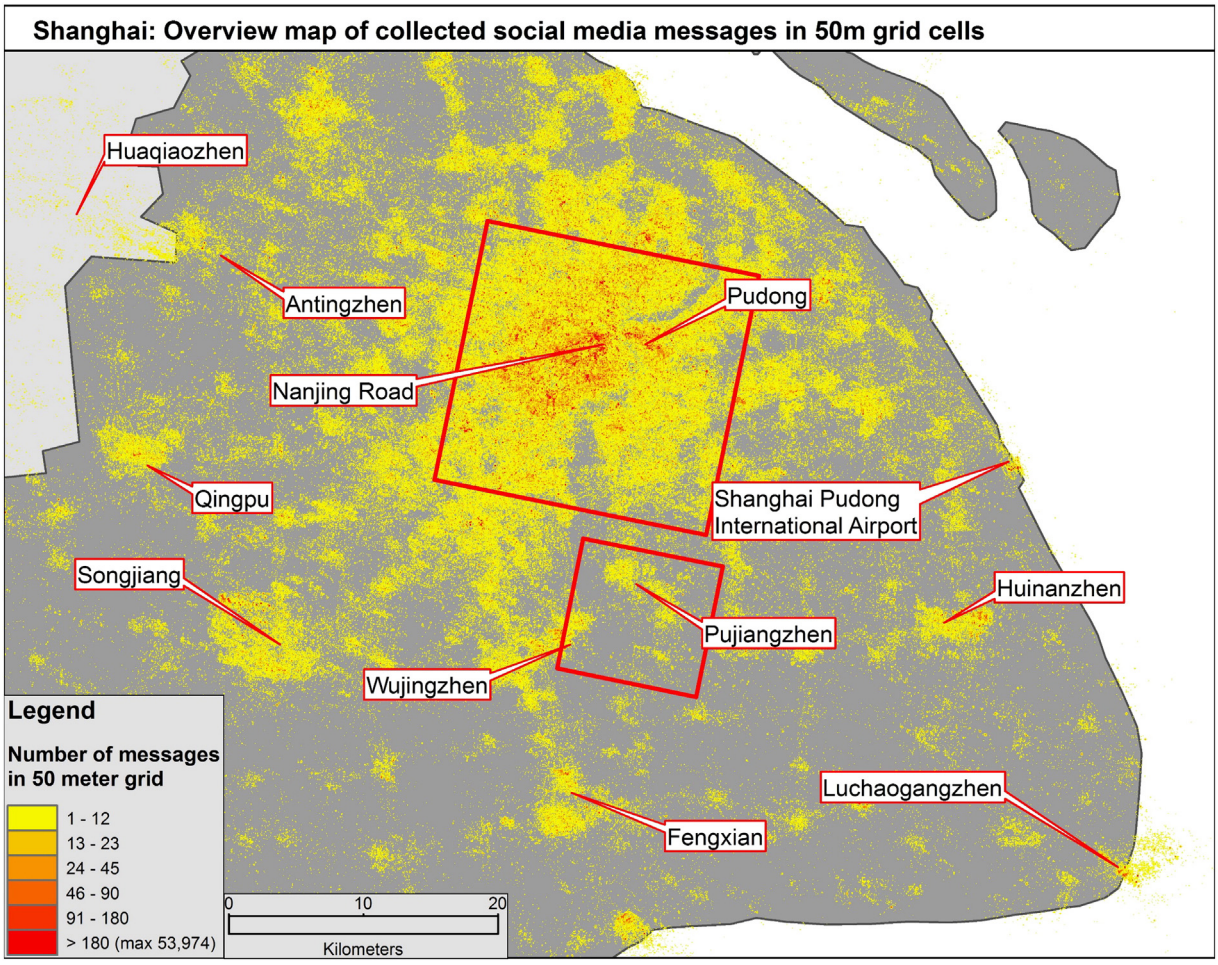

Fig. 4. Gridded mobile social media messages in Shanghai at 50 m cells. The entire metropolitan area is covered and clusters and patches of messages are visible on the map. The center of Shanghai is in the large red square and also covered with the mentioned built-up detection using SAR. The small red square is the suburb Pujiangzhen and an example area of a patch of messages. (For interpretation of the references to color in this figure legend, the reader is referred to the web version of this article.)

Changes in the infrastructure and built-up environment are due to long-term human activity but do not indicate the status of these areas; if they are accepted and used by people or not. The color composite image in Fig. 3 is a visualization of built-up structural changes.

4.2. Concentration and patterns of human activity

The gridded social media messages appear as a raster of 2417 columns and 3115 rows, with each cell representing the number of messages counted in that specific squared area of 50 m, Fig. 4. This representation is purely for qualitative purposes and serves as an illustration that shows message point densities. The cells with zero message counts within half a year are transparent in this figure. The maximum count of messages within half a year for a single cell is 53,000 messages. We selected a color grading system that approximately doubles each class in size until 180 messages are reached; indicating that on average, at least one message was sent from this particular area every day during the half-year observation period.

Gridding and color grading a sample of ~3.6 million messages reveal patterns in the distribution of messages with one major message cluster at the center of Shanghai. This area contains popular shopping streets such as Nanjing road, the business district, and the Bund. On the other side of the river is Pudong with its high-rise buildings and dense built-up environment. These areas have cells with far >180 messages in six months and are color coded in red.

Moving away from the center, there are agglomerations of messages in the suburbs and towns of Antingzhen, Qingpu, Songjiang, Wijingzhen, Pujiangzhen, Fengxian, Luchaogangzhen and Huinanzhen, Fig. 4. 'Zhen' (镇) is translated as town/small town and the smallest administrative unit in China. This suggests that the presence of a built-up area is associated with sent and received messages. If there are messages then this area is probably an urban built-up environment, a plausible correlation.

Looking at the areas that are non-urban such as water bodies and agricultural land; messages sent from these areas are rare and spread out. We see the message sent from ships along the river in the center of Shanghai. Those are most likely from ferries on the river.

4.3. Visually combining urban built-up change and human activity patterns

In the previous section, we have established that social media messages - as an indicator of human activity -appear in agglomerations likely within urban areas. Urban areas with high coherence such as the center of Shanghai, with its high buildings, show a high number of SMM. Built-up density seems to be correlated with human activity.

Figure 5shows side-by-side views of the area around the 2010 World Exhibition site in Shanghai. On the left is a built-up change detection composition image. On the right, the same area is shown with an SMM layer superimposed. In fig. 5, to the right, SMM grid cells with 12 or fewer messages within half a year of observation; for visualization purposes, were made transparent. The blue color in the change detection composition image indicates that change stopped in 2012. Red in the layer for social media messages means a high number of messages. In Pudong and the center of Shanghai, the number of messages often

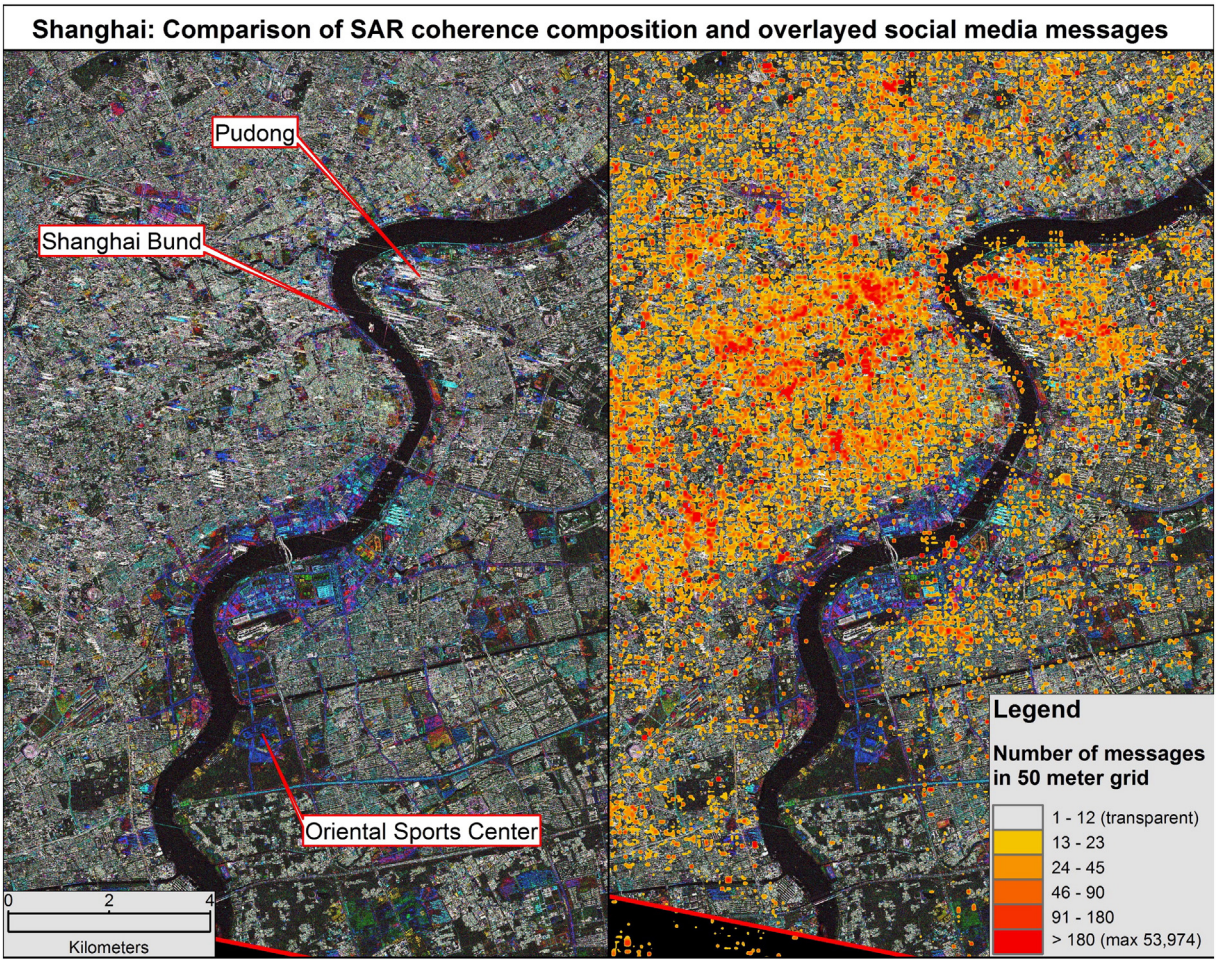

Fig. 5. Side by side, comparison of built-up detection (left) and same image superimposed with SMM (right). (For interpretation of the references to color in this figure legend, the reader is referred to the web version of this article.)

reaches 180 and more. The grid cell with the highest number of recorded messages is also in this area.

The selected subset area of fig. 5 reveals that today the EXPO area is a brownfield, 'ghost town like' area along the river. Indications for this statement are a) except for the river and the park around the Oriental sports center the entire frame appears bright in the coherence composition image. This means a complete coverage of built-up structures, and b) Variations in the SMM density indicate that human activity does not happen uniformly over the same built-up area. Especially the bright blue area of the ex 2010 World exhibition site experiences no messages but is surrounded by higher SMM density.

This discovery is important for two reasons: First, there is a sharp edge in message density following the northern edge of the EXPO area. Second, south of the area we see an increased number of messages that is embedded in a built-up environment and more or less surrounded by SMM. The same is true for the Oriental Sports Center. However, we also see a decrease of SMM from the city center. Both data sets, unfortunately, do not cover exactly the same period.

Fig. 6 demonstrates a case where built-up matches human activity inferred from SMM, showing the direct overlay for the towns of Pujiangzhen und Wujingzhen south of the city center. The overlay with SMM fits very well to the built-up area below it. These two small towns (zhen) are examples of urban areas fully covered with human activity.

Special cases are the Shanghai Pudong International Airport as visible in Fig. 4 and Fig. 7. Messages are centered on the terminal buildings with only a few messages collected from the airfield. A number of messages are concentrated in the area between the two opposing terminals and runways. People transiting through the airport are sending messages about their travels, thus higher message density in these areas.

The overall result is that we can visually see that there might be a correlation between built-up and density of SMM.

4.4. Quantifying what we see

Quantitative evaluation of the method described in Section 3.3 results in a 72.50% overall matching between urban and social media messages for 400 m cells, a coherence threshold of 0.5 and a reference message count of six per 1 ha per 180 days, see Fig. 8, using the mean of the four most recent coherence images for matching. A visual comparison of our results to satellite images (as ground truth) reveals that a coherence threshold of 0.5 represents built-up areas very well, but with a slight underestimation. Six SMMs per half year for 1 ha are a suitable correspondence to the measurement of monthly active users – an average of one message per month. This overall match is scale dependent, e.g. if the cell size is increased to 2000 m and the coherence threshold to 0.55 and the number of messages per reference area to 40, then the match increases to 90.443%. At this larger level of aggregation, only the areas with high message density are taken at the core of the city. This classifies a much smaller area in the city center as built-up areas and human activity and the surrounding areas remain in the case 4 class. This granularity neglects variation within built-up areas and requires a lower coherence threshold, thus increased matching occurs with increased cell size.

A 2-by-2 contingency table (Table 2) shows the distribution of matches and mismatches, an analysis of the 9753 400 m cells indicates

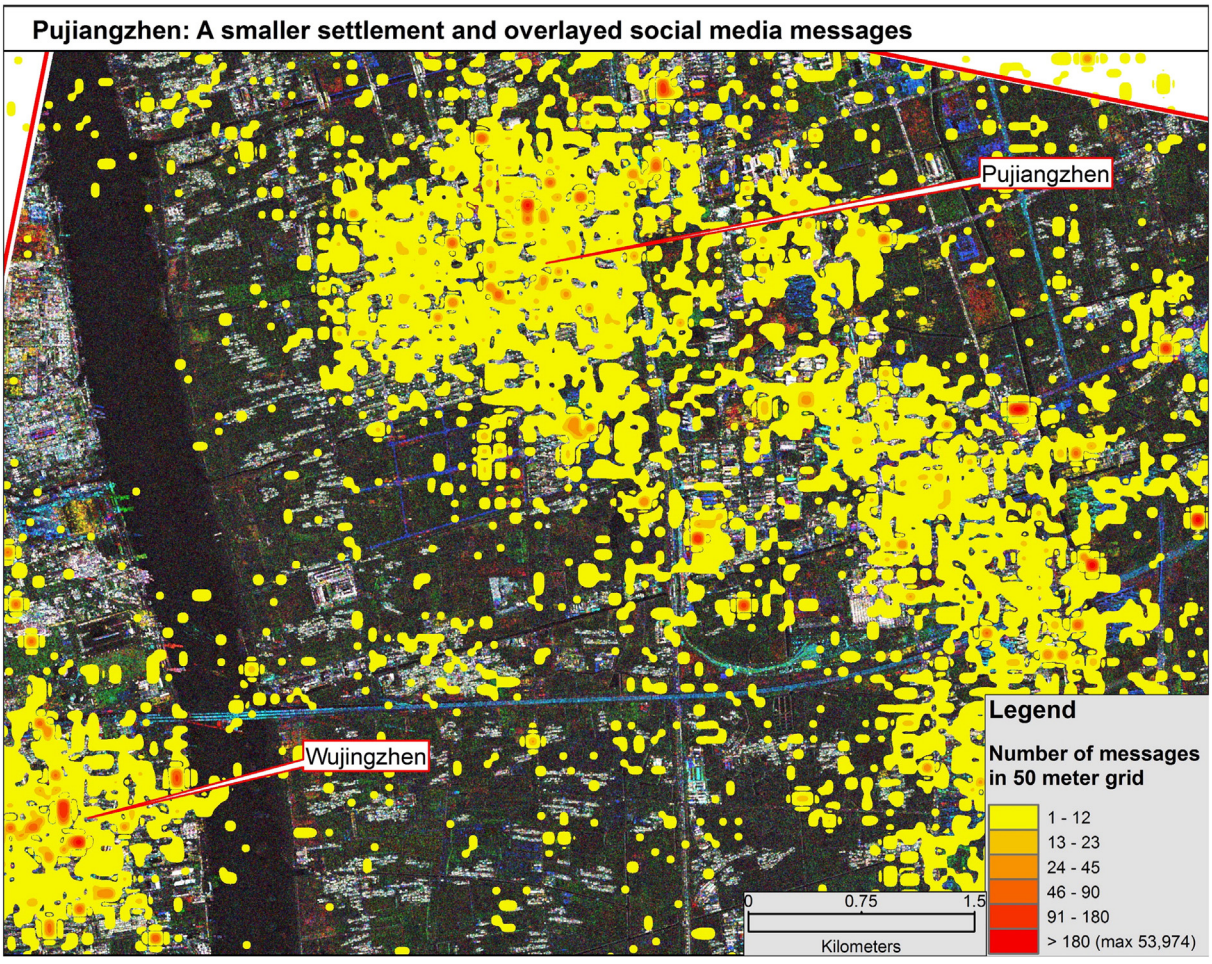

Fig. 6. Visual overlay of SAR coherence change detection and gridded social media messages in Pujiangzhen. (For interpretation of the references to color in this figure legend, the reader is referred to the web version of this article.)

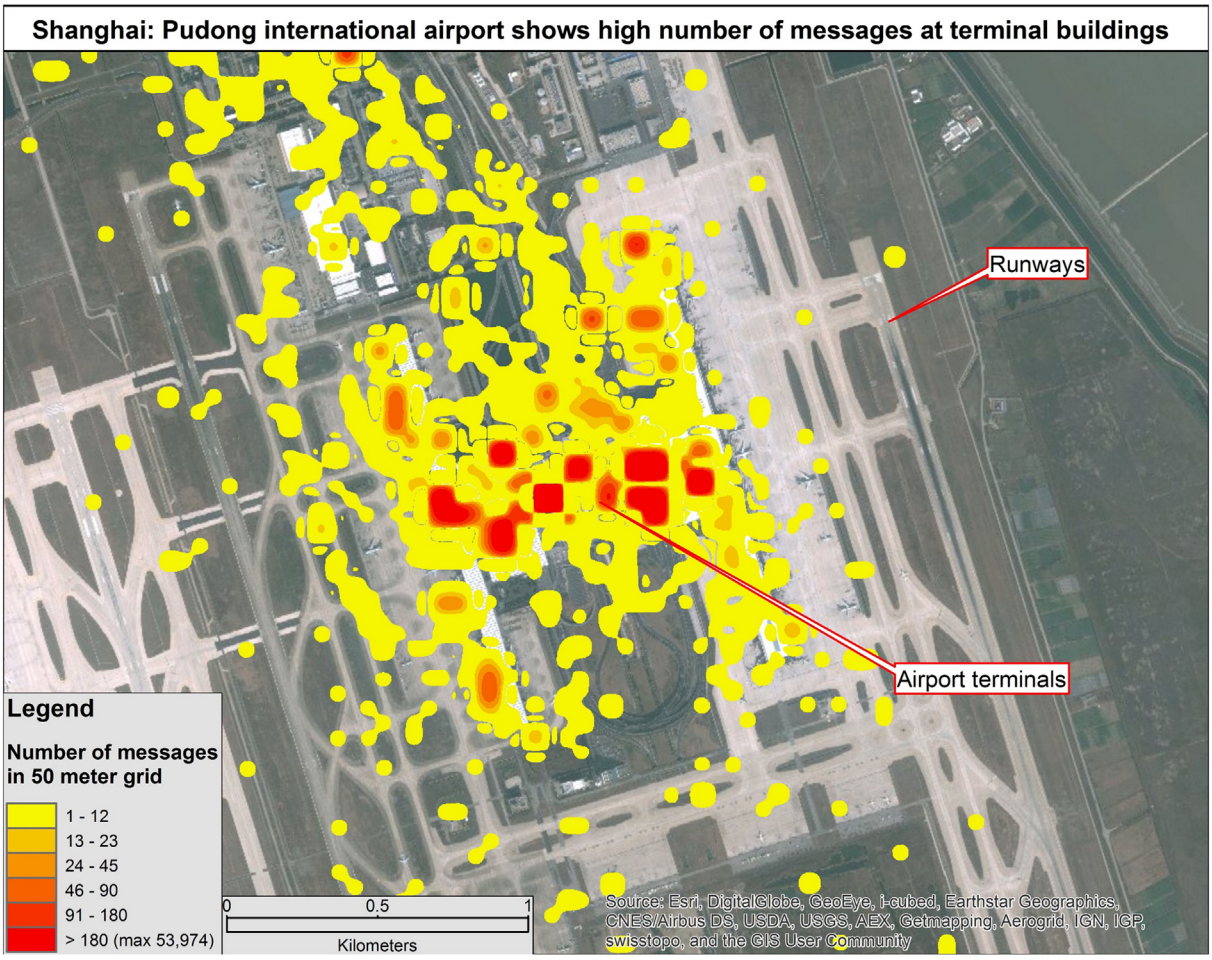

Fig. 7. Social media messages of Sina Weibo at the Pudong International Airport in Shanghai. (For interpretation of the references to color in this figure legend, the reader is referred to the web version of this article.)

that 36.5% (3560) of the area is comprised of built-up areas; 68.85% (1510) of this area also experiences human activity given the volume of SMM. Additionally, 39.08% of all SMM was identified to be in non-built-up areas. We recorded the existence of built-up (1) and SMM (1) areas as well as areas of no built-up (0) and SMM (0). A Chi-square test at significance level α of 0.05 gives a p-value of <0.001. Therefore, we can infer that there is a correlation between built-up areas and human activity.

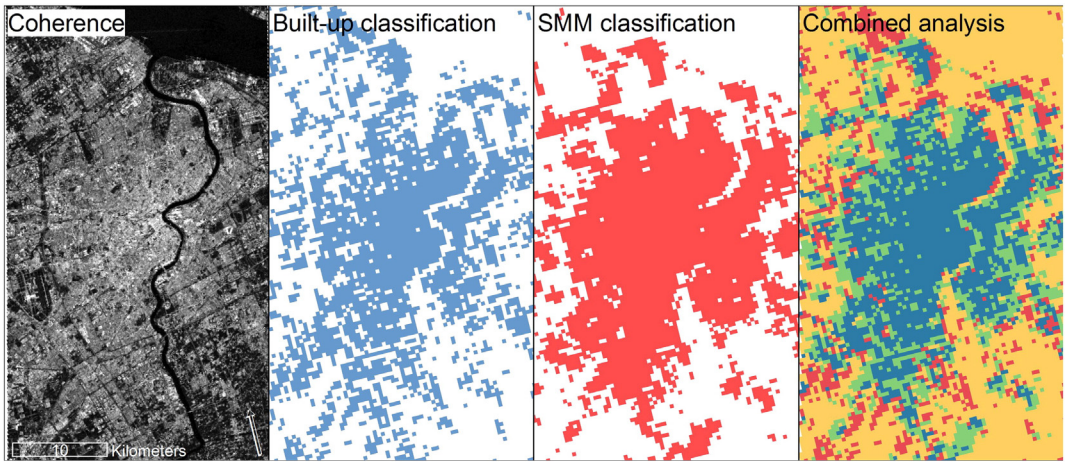

Fig. 8. The coherence image (left) shows areas of high coherence in white and low coherence in black. The map to the right is the binary classification of the image at a coherence threshold of 0.5; areas over this threshold are colored in blue. The Classification of social media messages is shown in the third frame at a threshold of 96 messages per 180 days per 400 m grid cells, colored in red. Derived from these two classifications is combination result of all four cases (see Table 2 and Fig. 9 as well) which is illustrated in the last frame, where blue (case 1) represents high built-up and high SMM, green (case 2) low built-up but high SMM, red (case 3) high built-up but low SMM, and yellow (case 4) low built-up and low SMM. (For interpretation of the references to color in this figure legend, the reader is referred to the web version of this article.)

Table 2
2-By-2 confusion Matrix with 9753 classified raster cells at 400 m.

Social Media Messages \ Built-up area	1	0	sum
1	Case 1: 2451	Case 2: 1572	4023
0	Case 3: 1109	Case 4: 4621	5730
sum	3560	6193	9753

Fig. 9 shows examples of classified areas. A: This is the central district of Shanghai with the business district in Pudong. The extent is dominated by blue pixels, which indicate a match between the existence of built-up areas and human activity. The green color denotes areas that are non-built-up areas but with human activity. There is ferry traffic between the sides of the river and tourist boats along it; people might take the opportunity when moving on or by the water to take pictures or post messages on Weibo. The second Extent (B) is a little further upstream, the river is classified as a non-built-up area without human activity (yellow). Right in the center of the frame is the Oriental Sports Center (three blue squares) with a park on the west side without human activity (yellow); the same park area extends to the east with human activity (green). The third row (C) shows an industrial complex (red) in the north of the city. The last row is an overview map; all classifications areas are comparable to the satellite image seen on the left.

From the examples in Fig. 9 we can see that the extracted built-up information from remote sensing as well as the human activity information from social media data are not randomly spread, but rather clustered. Completely dispersed built-up areas and human activity data would result in a checkerboard-like appearance. The spatial pattern, however, shows areas of both high and low values of built-up areas and human activity are clustered, and pattern of positive spatial autocorrelation. The degree of 'clusteredness'/grouping of values can be expressed as a Moran's I value. The range of this value extends from −1 (dispersed) to 1 (clustered). For our built-up areas classification scheme, a Moran's I value of 0.475 (p-value: 0.0001) at 400 m cell size was obtained. Built-up areas appear as clusters regardless of size or location. Human activity is also clustered, SMM are not randomly dispersed over the entire AOI but appear in groups and patches. This visual observation is supported by a Moran's I of 0.648 (p-value: 0.0001) for the same image extent as the built-up areas classification. We conclude that both data sets have an inherent, non-random spatial clustering pattern, conforming to our expectations. This pattern is scale dependent since built-up areas were classified into two discrete classes thus decreasing clustering. The clustering of SMM increases when classified into two discrete classes at 400 m while unclassified SMM show the highest degree of dispersion.

5. Conclusion

We have demonstrated an approach to achieve enhanced urban analysis by combining data from remote sensing and social media. We have shown the basic processing flow to generate coherence composition images to visualize changes in the built-up environment. Human activity was derived from social media messages which were gridded into 50 m cells and superimposed on top of the coherence images. To quantify the results, we aggregated and classified the results from remote sensing and social media into a combined layer at 400 m cell size to show the correlation of built-up environment and human activity. The proposed approach provides an enhanced interpretation of urban dynamics.

A simplified guideline for classifying areas is shown in the 2-by-2 matrix in Table 1 while the classification results are shown in Table 2. We found it possible to identify four different classes by looking at the built-up and social media message density. We found that the existence of human activity expressed by social media messages correlates with urban built-up areas. Fig. 9, is our core finding, showing the four classes of areas derived from the combined layer. Pudong as the business district of Shanghai has a high density of social media messages. The Oriental Sports Centre is an example of a single building complex, with both a high density of built-up and high human activity, while the surrounding areas have low built-up and low human activity.

We used these data sets because they are readily accessible. The social media messages from Sina Weibo are a rich source of information, with a significant market share and widely used across China. However, there is a set of limitation that are mentioned in Section 1.2 and in the science article (Ruths & Pfeffer, 2014). Example we do not know who is using the network and what percentage of the actually human activity in that area the SMM resemble. Only people with mobile devices are considered. From those, only users that have this application installed and use it at least monthly are considered. Additionally, only downloadable messages via the open API are included in our experiment – the biases introduced by Sina Weibo are unclear, too. The assumption is that younger and middle-aged people most likely are active on this platform. However, our premise was to detect instant human activity by taking a subset of the population. We did not attempt to estimate population. Human activity for an entire municipal area can be visualized and statements about activity patterns and certain neighborhoods can be made.

Other limitations that cannot be changed are the positioning accuracy of the mobile devices and we cannot say with 100% certainty, that we collected all the messages sent during the observation period with our search algorithm. Built-up density estimation with coherence images poses the problem of inconsistencies due to layover and shadow effects from high-rise buildings. However, because we are working on aggregated, lower resolution data, we believe that these limitations are not significant for our analysis. The positioning accuracy of SMM is already an improvement over census data, and a sample size of 3.8 million messages in a 24 million people city might be considered as indicative of human activity.

The non-concurrence of the two datasets, built-up information from 2012 and human activity information from 2014, results in errors and ambiguities. The population grew by 1.9% and the built-up environment certainly changed in the two-year gap between the datasets. While it would be desirable to have data that covers the same timespan the introduced uncertainties cannot be evaded with the data at hand.

Future work will focus on aspects that can be changed to improve the results. First, we aspire to get two data sets that definitely cover the same time period and area. This will allow us to perform a time series not only for the built-up information derived from SAR but also to make the human activity layer time sensitive to show urban dynamics of e.g. newly constructed neighborhoods. Microwave remote sensing images deliver a very suitable source of data to delineate urban areas. Using multiple – a time series stack – of images allows the identification

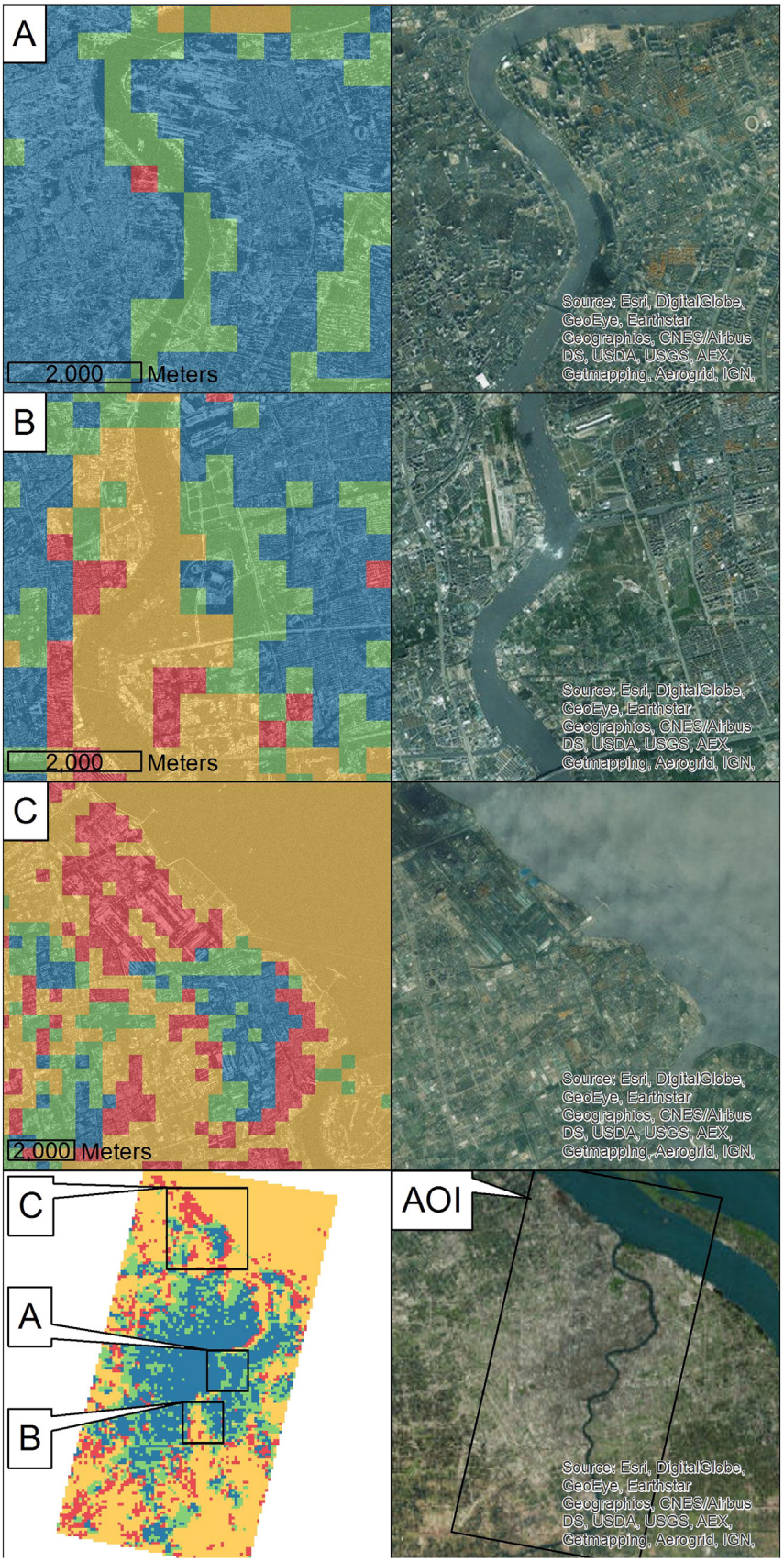

Fig. 9. Subsets of the classification: Blue: Built-up areas and human activity detected, Red: Built-up areas detected but no human activity, Green: No built-up areas detected but human activity and Yellow: No built-up areas or human activity detected. A: The very center of Shanghai with the Pudong business district, B: The Oriental Sports Center (covered by 3 blue squares) its` surrounding park and the HuangPu river, C: An industrial area (marked with red cells) in the northern part of the city. At the bottom is an overview map (top square = C, middle = A and bottom = B). (For interpretation of the references to color in this figure legend, the reader is referred to the web version of this article.)

of changes over time. In future applications, we aim to get SAR data from freely available sources such as Sentinel-1 from ESA and incorporate e.g. persistent scatter point density and height information to enhance the built-up density.

Acknowledgements

This work is financially supported by the National Natural Science Foundation of China (grant no. 61331016 and 41174120), and the German Academic Exchange Service (DAAD).

References

Ao, J., Zhang, P., & Cao, Y. (2014). Estimating the locations of emergency events from twitter streams. *Procedia Computer Science*, *31*, 731–739. http://dx.doi.org/10.1016/j.procs.2014.05.321.

Boldt, M., & Schulz, K. (2012). *Change detection in high resolution SAR images: Amplitude based activity map compared with the CoVAmCoh analysis* (pp. 3803–3806). 2012 IEEE International Geoscience and Remote Sensing Symposium. IEEE. http://dx.doi.org/10.1109/IGARSS.2012.6350584.

Broniatowski, D. A., Paul, M. J., & Dredze, M. (2014). Twitter: Big data opportunities. *Science*, *345*(6193), 148. http://dx.doi.org/10.1126/science.345.6193.148-a.

Brunner, D., Lemoine, G., Bruzzone, L., & Greidanus, H. (2010). Building height retrieval from VHR SAR imagery based on an iterative simulation and matching technique. *IEEE Transactions on Geoscience and Remote Sensing*, *48*(3), 1487–1504. http://dx.doi.org/10.1109/TGRS.2009.2031910.

Burton, S. H., Tanner, K. W., Giraud-Carrier, C. G., West, J. H., & Barnes, M. D. (2012). Right time, right place" health communication on twitter: Value and accuracy of location information. *Journal of Medical Internet Research*, *14*(6). http://dx.doi.org/10.2196/jmir.2121.

Calabrese, F., Colonna, M., Lovisolo, P., Parata, D., & Ratti, C. (2010). Real-time urban monitoring using cellular phones: A case-study in Rome. *IEEE Transactions on Intelligent Transportation Systems*, *12*(1), 1–11. http://dx.doi.org/10.1109/tits.2010.2074196.

Calabrese, F., Diao, M., Di Lorenzo, G., Ferreira, J., & Ratti, C. (2013). Understanding individual mobility patterns from urban sensing data: A mobile phone trace example. *Transportation Research Part C: Emerging Technologies*, *26*, 301–313. http://dx.doi.org/10.1016/j.trc.2012.09.009.

Candia, J., González, M. C., Wang, P., Schoenharl, T., Madey, G., & Barabási, A. -L. (2008). Uncovering individual and collective human dynamics from mobile phone records. *Journal of Physics A: Mathematical and Theoretical*, *41*. http://dx.doi.org/10.1088/1751-8113/41/22/224015 224015–11.

Carter, M. A. (2013). Third party observers witnessing cyber bullying on social media sites. *Procedia - Social and Behavioral Sciences*, *84*, 1296–1309. http://dx.doi.org/10.1016/j.sbspro.2013.06.747.

Chen, S., Zhang, H., Lin, M., & Lv, S. (2011). *Comparision of microblogging service between Sina Weibo and Twitter. Proceedings of 2011 International Conference on Computer Science and Network Technology4*. (pp. 2259–2263). IEEE. http://dx.doi.org/10.1109/ICCSNT.2011.6182424.

Chi, H., Sun, G., & Ling, F. (2009). Urban dynamic change detection in southeastern China based on interferometric SAR. *Urban Remote Sensing Event*, *2009*(3), 1–9. http://dx.doi.org/10.1109/IGARSS.2009.5417796.

China Data Center (2013). China 2010 township population census data with GIS maps. http://chinadatacenter.org/DataCategory/DataCategoryContent.aspx?type=2&id=1624

Cohen, R., & Ruths, D. (2013). *Classifying political orientation on Twitter: It's not easy!* (pp. 91–99). Seventh International AAAI Conference on Weblogs … http://www.aaai.org/ocs/index.php/ICWSM/ICWSM13/paper/viewFile/6128/6347\npapers3://publication/uuid/3532F9EA-312A-4F8E-83C3-6369D71D2171.

Crooks, A., Pfoser, D., Jenkins, A., Croitoru, A., Stefanidis, A., Smith, D., et al. (2015). Crowdsourcing urban form and function. *International Journal of Geographical Information Science*, *29*(5), 720–741. http://dx.doi.org/10.1080/13658816.2014.977905.

Ding, L., Fan, H., & Meng, L. (2015). Understanding taxi driving behaviors from movement data. In F. Bacao, M. Y. Santos, & M. Painho (Eds.), *Lecture Notes in Geoinformation and Cartography. 217*. (pp. 219–234). Springer. http://dx.doi.org/10.1007/978-3-319-16787-9_13.

Esch, T., Taubenböck, H., Felbier, A., Heldens, W., Wiesner, M., & Dech, S. (2012). *Monitoring of global urbanization-time series analyses for mega cities based on optical and SAR data* (pp. 21–25). Proceedings of the 2nd International Workshop on Earth Observation and Remote Sensing Applications, EORSA 2012. IEEE. http://dx.doi.org/10.1109/EORSA.2012.6261127.

Esch, T., Taubenböck, H., Roth, A., Heldens, W., Felbier, A., Thiel, M., et al. (2012). TanDEM-X mission—New perspectives for the inventory and monitoring of global settlement patterns. *Journal of Applied Remote Sensing*, *6*(1), 61701–61702. http://dx.doi.org/10.1117/1.JRS.6.061702.

Esch, T., Marconcini, M., Felbier, A., Roth, A., Heldens, W., Huber, M., et al. (2013). Urban footprint processor-Fully automated processing chain generating settlement masks from global data of the TanDEM-X mission. *IEEE Geoscience and Remote Sensing Letters*, *10*(6), 1617–1621. http://dx.doi.org/10.1109/LGRS.2013.2272953.

Fédération internationale de natation (2010). Shanghai oriental sports center 14th FINA world championships - Shanghai 2011. http://www.shanghai-fina2011.com/13/2010/0708/5.html

Fu, K. W., & Chau, M. (2013). Reality check for the Chinese microblog space: A random sampling approach. *PLoS ONE*, *8*(3). http://dx.doi.org/10.1371/journal.pone.0058356.

Gao, S. (2015). Spatio-temporal analytics for exploring human mobility patterns and urban dynamics in the mobile age. *Spatial Cognition and Computation*, *15*(2), 86–114. http://dx.doi.org/10.1080/13875868.2014.984300.

Goodchild, M. F. (2007). Citizens as sensors: The world of volunteered geography. *GeoJournal*, *69*(November), 211–221. http://dx.doi.org/10.1007/s10708-007-9111-y.

Guo, Y., & Goh, D. H. -L. (2014). "I have AIDS": Content analysis of postings in HIV/AIDS support group on a Chinese microblog. *Computers in Human Behavior*, *34*, 219–226. http://dx.doi.org/10.1016/j.chb.2014.02.003.

He, M., & He, X. F. (2009). *Urban change detection using coherence and intensity characteristics of multi-temporal SAR imagery. 2009 2nd Asian-Pacific Conference on Synthetic Aperture Radar1*. (pp. 840–843). http://dx.doi.org/10.1109/APSAR.2009.5374186.

Huang, Q., Yang, X., Gao, B., Yang, Y., & Zhao, Y. (2014). Application of DMSP/OLS nighttime light images: A meta-analysis and a systematic literature review. *Remote Sensing*, *6*(8), 6844–6866. http://dx.doi.org/10.3390/rs6086844.

Jenkins, A., Croitoru, A., Crooks, A. T., & Stefanidis, A. (2016). Crowdsourcing a collective sense of place. *PLoS ONE*, *11*(4), 1–20. http://dx.doi.org/10.1371/journal.pone.0152932.

Jin, M. S., Kessomkiat, W., & Pereira, G. (2011). Satellite-observed urbanization characters in shanghai, China: Aerosols, urban heat island effect, and land–atmosphere interactions. *Remote Sensing*, *3*(12), 83–99. http://dx.doi.org/10.3390/rs3010083.

Kang, C., Sobolevsky, S., Liu, Y., & Ratti, C. (2013). *Exploring human movements in Singapore. Proceedings of the 2nd ACM SIGKDD International Workshop on Urban Computing - UrbComp r'131*. http://dx.doi.org/10.1145/2505821.2505826.

Kase, S. E., Bowman, E. K., Al Amin, M. T., & Abdelzaher, T. (2014). Exploiting social media for Army operations: Syrian crisis use case. In B. D. Broome, D. L. Hall, & J. Llinas (Eds.), *SPIE sensing Technology + Applications* (pp. 91220D). International Society for Optics and Photonics. http://dx.doi.org/10.1117/12.2049701.

Lansley, G., & Longley, P. A. (2016). The geography of twitter topics in London. *Computers, Environment and Urban Systems*, *58*, 85–96. http://dx.doi.org/10.1016/j.compenvurbsys.2016.04.002.

Lazer, D., Kennedy, R., King, G., & Vespignani, A. (2014). The parable of google flu: Traps in big data analysis. *Science*, *343*(14 March 2014), 1203–1205. http://dx.doi.org/10.1126/science.1248506.

Li, X., & Li, D. (2014). Can night-time light images play a role in evaluating the Syrian crisis? *International Journal of Remote Sensing*, *35*(18), 6648–6661. http://dx.doi.org/10.1080/01431161.2014.971469.

Lillesand, T., Kiefer, R. W., & Chipman, J. (2015). *Remote sensing and image interpretation* (7th ed.).

Liu, W., & Yamazaki, F. (2011). Urban monitoring and change detection of central Tokyo using high-resolution X-band SAR images. *IEEE International Geoscience and Remote Sensing Symposium*, *2011*, 2133–2136. http://dx.doi.org/10.1109/IGARSS.2011.6049587.

Liu, Y., Wang, F., Xiao, Y., & Gao, S. (2012). Urban land uses and traffic "source-sink areas": Evidence from GPS-enabled taxi data in Shanghai. *Landscape and Urban Planning*, *106*(1), 73–87. http://dx.doi.org/10.1016/j.landurbplan.2012.02.012.

Liu, Y., Sui, Z., Kang, C., & Gao, Y. (2014). Uncovering patterns of inter-urban trip and spatial interaction from social media check-in data. *PLoS ONE*, *9*(1), e86026. http://dx.doi.org/10.1371/journal.pone.0086026.

Liu, Y., Liu, X., Gao, S., Gong, L., Kang, C., Zhi, Y., et al. (2015). Social sensing: A new approach to understanding our socioeconomic environments. *Annals of the Association of American Geographers*, *105*(3), 512–530. http://dx.doi.org/10.1080/00045608.2015.1018773.

Louail, T., Lenormand, M., Cantu Ros, O. G., Picornell, M., Herranz, R., Frias-Martinez, E., et al. (2014). From mobile phone data to the spatial structure of cities. *Scientific Reports*, *4*, 5276. http://dx.doi.org/10.1038/srep05276.

Perissin, D., & Wang, T. (2011). Time-series InSAR applications over urban areas in China. *IEEE Journal of Selected Topics in Applied Earth Observations and Remote Sensing*, *4*(1), 92–100. http://dx.doi.org/10.1109/JSTARS.2010.2046883.

Reades, J., Calabrese, F., Sevtsuk, A., & Ratti, C. (2007). Cellular census: Explorations in urban data collection. *IEEE Pervasive Computing*, *6*(3), 30–38. http://dx.doi.org/10.1109/MPRV.2007.53.

Reades, J., Calabrese, F., & Ratti, C. (2009). Eigenplaces: Analysing cities using the space-Time structure of the mobile phone network. *Environment and Planning. B, Planning & Design*, *36*(5), 824–836. http://dx.doi.org/10.1068/b34133t.

Rui, H., Liu, Y., & Whinston, A. (2013). Whose and what chatter matters? The effect of tweets on movie sales. *Decision Support Systems*, *55*(4), 863–870. http://dx.doi.org/10.1016/j.dss.2012.12.022.

Ruths, D., & Pfeffer, J. (2014). Social media for large studies of behavior. *Science*, *346*(6213), 1063 http://www.pfeffer.at/science2014.pdf. Accessed 22 December 2014.

Shanghai Bureau of Statistics (2015). Total households, population, density of registered population and life expectancy (1978–2014). *Shanghai Statistical Yearbook* http://www.stats-sh.gov.cn/tjnj/nje15.htm?d1=2015tjnje/E0201.htm. Accessed 26 August 2016.

Stefanidis, A., Crooks, A., & Radzikowski, J. (2013). Harvesting ambient geospatial information from social media feeds. *GeoJournal*, *78*(2), 319–338. http://dx.doi.org/10.1007/s10708-011-9438-2.

Sutton, P., Roberts, D., Elvidge, C., & Baugh, K. (2010). Census from heaven: An estimate of the global human population using night-time satellite imagery. *International Journal of Remote Sensing*, *22*(16), 3061–3076. http://dx.doi.org/10.1080/01431160010007015.

Taylor, P. J. (2001). GaWC - A brief guide to quantitative data collection. http://www.lboro.ac.uk/gawc/guide.html

Tufekci, Z. (2014). *Big questions for social media big data: Representativeness, validity and other methodological pitfalls* (pp. 10). ICWSM '14: Proceedings of the 8th International AAAI Conference on Weblogs and Social Media. http://arxiv.org/abs/1403.7400.

United Nations Population Division (2011). World urbanization prospects, the 2011 revision. http://esa.un.org/unpd/wup/index.htm

Wadge, G. (2002). Atmospheric models, GPS and InSAR measurements of the tropospheric water vapour field over Mount Etna. *Geophysical Research Letters*, *29*(19), 1905. http://dx.doi.org/10.1029/2002GL015159.

Sina Weibo (2014). The "nearby timeline" API request 2/place/nearby timeline - 微博API. http://open.weibo.com/wiki/2/place/nearby_timeline

Widener, M. J., & Li, W. (2014). Using geolocated Twitter data to monitor the prevalence of healthy and unhealthy food references across the US. *Applied Geography*, *54*, 189–197. http://dx.doi.org/10.1016/j.apgeog.2014.07.017.

Woodhouse, I. (2006). *Introduction to microwave remote sensing*. CRC Press.

Xiao, Y., & Zhan, Q. (2009). A review of remote sensing applications in urban planning and management in China. *Joint Urban Remote Sensing Event*, *2009*, 1–5. http://dx.doi.org/10.1109/URS.2009.5137653.

Xu, Z. -W., Wu, J., & Wu, Z. -S. (2004). A survey of ionospheric effects on space-based radar. *Waves in Random Media*, *14*(2), S189–S273. http://dx.doi.org/10.1088/0959-7174/14/2/008.

Yifang, B., Alexander, J., & Gamba, P. (2013). Spaceborne SAR data for global urban mapping at 30 m resolution using a robust urban extractor. *ISPRS Journal of Photogrammetry and Remote Sensing*. http://dx.doi.org/10.1016/j.isprsjprs.2014.08.004.

Zook, M., & Poorthuis, A. (2014). Offline brews and online views: Exploring the geography of beer tweets. In M. Patterson, & N. Hoalst-Pullen (Eds.), *The Geography of Beer (pp. 201–209)*. Springer. http://dx.doi.org/10.1007/978-94-007-7787-3.